Noninvasive Assessment of Regional Cardiac Adenosine Using Positron Emission Tomography

Andreas Deussen, Michael Henrich, Kurt Hamacher, Mathias M. Borst, Hans Herzog, Heinz H. Coenen, Gerhard Stöcklin, Ludwig E. Feinendegen and Jürgen Schrader

Zentrum für Physiologie, Heinrich-Heine-Universität Düsseldorf, Düsseldorf, Germany, Institut für Medizin and Institut für Chemie 1, Forschungszentrum Jülich, Jülich, Germany

One of the early metabolic changes associated with myocardial ischemia is the breakdown of adenine nucleotides resulting in the enhanced production of adenosine. In order to image regional cardiac adenosine by positron emission tomography (PET) the enzymatic conversion of adenosine into [^{11}C]-S-adenosylhomocysteine ([^{11}C]SAH) was used in the presence of ^{11}C-labeled homocysteine thiolactone (adenosine + [^{11}C] − homocysteine → [^{11}C] − SAH + H_2O). Following production of an experimental coronary constriction in anesthetized dogs carrier added 1-[^{11}C]-D,L-homocysteine thiolactone (5–27 mCi, 30 mg/kg) was infused over 1 min. This intervention, while hemodynamically ineffective, increased the plasma homocysteine concentration from 2.5 to 306 μM, which thereafter declined with a $T_{½}$ of 28 min to 97 μM after 60 min. During the first minutes following infusion of [^{11}C] homocysteine, the radioactivity concentration in the blood pool, the nonischemic and the ischemic myocardium were similar. Between 20 and 60 min, however, the regional radioactivity concentration was highest in the perfusion area of the stenosed vessel: 6.6% compared to 5.2 and 5.2% of the injected dose per 1 l tissue. The elevated radioactivity concentration was strictly confined to the perfusion area of the occluded artery. Using [^{35}S]-L-homocysteine (20 μCi; 30 mg/kg) chromatographic separation of SAH in tissue extracts confirmed that the radioactivity accumulation was due to trapping of adenosine in the cellular SAH-pool. These experiments provide first evidence that 1-[^{11}C]homocysteine thiolactone can be successfully used to assess regional adenosine formation in the heart with PET via measurement of [^{11}C] SAH accumulation.

J Nucl Med 1992; 33:2138–2144

During cardiac ischemia, adenosine production from adenine nucleotides is increased (*1,2*) (Fig. 1). Isolated cell experiments show that adenosine production strictly depends on the oxygenation (*3*). Below a threshold-pO_2 of 3 Torr, the cellular rate of adenosine formation is significantly augmented and a function of the pO_2 reduction. Under in situ conditions, adenosine formation occurs in proportion to the impairment of the supply-to-demand ratio for oxygen (*4,5*), thus reflecting myocardial oxygenation.

During exertional angina in man, the coronary venous-arterial difference of adenosine was shown to increase (*6*). However, assessment of venous-arterial differences does not allow one to localize the underlying underperfusion. Furthermore, due to the complexities of adenosine transport and metabolism, the interpretation of these measurements remains controversial (*7*). Recently, our laboratory elaborated a new technique that circumvents most of the limitations of previous methods and permits a regional assessment of myocardial adenosine (*4,8*). It is based on the intracellular conversion of free adenosine into S-adenosylhomocysteine (SAH) by action of cytosolic SAH-hydrolase (adenosine + homocysteine → SAH + H_2O) (Fig. 1). Because SAH is not further metabolized or transported across the cellular membranes in the heart (*9,10*), its rate of tissue accumulation can be used as a measure of the free cytosolic adenosine concentration.

In the present study, we have extended the principles of the SAH- technique to measure enhanced levels of cardiac adenosine with positron emission tomography (PET). For this purpose, racemic 1-[^{11}C]-D,L-homocysteine thiolactone was synthesized and the distribution of the label was measured under conditions of myocardial underperfusion. The model chosen was the canine heart in situ with a critical epicardial vessel stenosis. This hemodynamic condition is associated with a pronounced adenosine production without critical diminution of energy rich phosphates and preservation of global cardiac function (*4*). We demonstrate that poststenotic adenosine production can sensitively and noninvasively be assessed with good spatial resolution. Because of adenosine's link to cardiac energy metabolism, this approach may also provide a novel index of tissue oxygenation.

METHODS

Seven dogs (20–25 kg) were anesthetized (sodiumpentobarbital 30 mg/kg i.v.), intubated and ventilated with a respirator (type

Received October 7, 1991; revision accepted June 11, 1992.
For reprints contact: Andreas Deussen, Zentrum für Physiologie, Heinrich-Heine-Universitat Düsseldorf, Moorenstr. 5, D-4000 Düsseldorf 1, Germany.

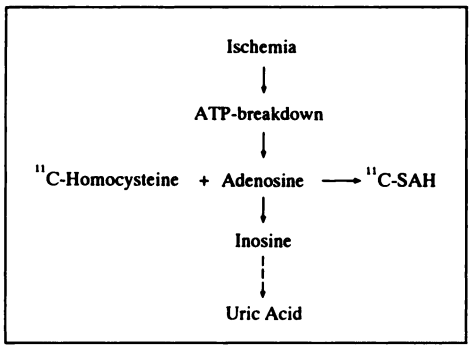

FIGURE 1. Mechanism of ischemic adenosine production in the heart. In the presence of ^{11}C-homocysteine, the label is trapped in the SAH fraction in proportion to the free adenosine concentration.

874/052, Braun, Melsungen, FRG). The right femoral artery and vein were cannulated for measurement of aortic blood pressure (P 23 ID, Statham, Gould, Oxnard, CA), blood sampling, volume substitution, and drug infusion. Heart rate was determined from the blood pressure recording. After thoracotomy and opening of the pericardium, a catheter was advanced into the left atrium via the appendage for later infusion of ^{99m}Tc-labeled albumin microspheres. A small side branch of the left circumflex coronary artery was retrogradely cannulated (20 g, Abbocath-T, Abbot, Ireland) for measurement of distal coronary pressure (P23 ID, Statham). Proximal to the cannulated side branch a circumferential constrictor device was placed around the circumflex artery for later narrowing of the vessel. Aortic and coronary blood pressure as well as heart rate were continuously recorded (R-56-54, Rikandenki-Kogyo, Tokyo, Japan).

To induce myocardial underperfusion, the constrictor device was adjusted to reduce distal coronary pressure to about 60/20 mmHg (systolic/diastolic). The degree of stenosis (judged by the aortic/distal coronary pressure difference) was maintained constant over the remaining experimental period. This experimental procedure was followed in six experiments. In one experiment the circumflex artery was left intact and ischemia was induced by ligation of a side branch of the left anterior descending coronary artery.

1-[^{11}C]-D,L-homocysteine thiolactone was synthesized as described recently (*11*). The labeling procedure was performed by the reaction of ^{11}C-carbon dioxide with α-lithiated S-(tetrahydropropan-2-yl)3-thiopropyl isonitrile, according to the reaction scheme shown in Figure 2. To enhance homocysteine plasma concentration, the ^{11}C-labeled homocysteine was supplied with unlabeled homocysteine to a final dose of 30 mg/kg (four experiments) and 10 mg/kg (two experiments). Five minutes after inducing the myocardial ischemia, the total yield of ^{11}C-labeled homocysteine, ranging between 5 and 27 mCi (supplemented to 10 or 30 mg/kg, respectively), was administered intravenously over 1 min. Data acquisition with a whole-body positron emission tomograph PC-4096-15WB (*12*) was started at the beginning of homocysteine infusion. The inplane resolution of reconstructed images was 7 mm measured as the full width at half maximum. Slice thickness was 6.5 mm.

Transmission scans were done with a rotating pin source containing 10 mCi of ^{68}Ge to correct for photon attenuation. Serial scans of 15 transversal cross-sections were acquired for 60 min. The acquisition time of the scans ranged from 15 sec to 10 min. Regions of interest were drawn manually in the various organs under study. These regions had a minimal distance of 1 cm from the border of the parenchymatous organs. In the case of the myocardium, the maximum profile was used in order to minimize the partial volume effect.

The radioactivity concentration in plasma and native blood sampled from the femoral artery was measured in a well-counter cross-calibrated to the PET camera. To objectify the underperfusion, at the end of each experiment, 1 mCi ^{99m}Tc-labeled albumine microspheres (10–90 μm diameter) was injected via the atrial catheter. Two minutes later the heart was arrested (saturated KCl i.v.), removed, washed in physiologic saline and cut in 2-cm thick slices parallel to the basis. Images of the regional ^{99m}Tc distribution in the slices were made in vitro using a gamma camera (Philips, Eindhoven, The Netherlands) with a low-energy, all-purpose collimator.

The specific incorporation of the homocysteine label into the SAH fraction was assessed in one additional experiment. Because of the short $T_{1/2}$ of the ^{11}C label and the time required for tissue extract separation by HPLC, [^{35}S]-L-homocysteine thiolactone in the presence of carrier DL-homocysteine thiolactone (total activity 20 μCi; total dose 30 mg/kg) was used under otherwise identical conditions. Transmural biopsies (88 ± 16 mg wet weight) were taken from the underperfused circumflex region with a high speed drill. Samples were directly transferred into liquid nitrogen and freeze dried (Lyovac GT 2, Leybold-Heraeus, Köln, Germany). After homogenization in perchloric acid, the neutralized extracts were used for measurement of homocysteine and SAH by HPLC, as described elsewhere (*4*). To determine the specific radioactivity of SAH, the fraction of column eluate containing SAH was sampled and the concentration of the ^{35}S-label was measured by routine liquid-scintillation spectrometry (PW 4700, Philips).

Homocysteine concentrations of plasma and tissue were measured enzymatically. After deproteinization of 0.4 ml plasma, 0.15 ml of the neutralized supernatant (10,000 g, 5 min) were mixed with 0.12 ml Tris-buffer (0.5 *M*, pH 8) and 30 μl dithioerythritol (100 m*M*), incubated at 37° C for 5 min and thereafter stored on ice. After addition of 75 μl of a charcoal suspension (KH_2PO_4 0.5 *M*, dithioerythritol 50 m*M*, dextran 2.5 mg/ml, charcoal 25 mg/ml, pH 7.4) samples were stored at 4° C for another 10 min and finally centrifuged (10,000 g, 5 min). Next, 100 μl of the above supernatant were mixed with 10 μl of the adenosine deaminase inhibitor EHNA (1 m*M*) and 20 μl adenosine (1 m*M*). Reaction was started by adding 20 μl (0.5 mg protein) of a cytosolic extract prepared from rat liver (SAH-hydrolase activity 14 nmol·min^{-1}·mg protein^{-1}). After incubation for 60 min at 37° C, the reaction

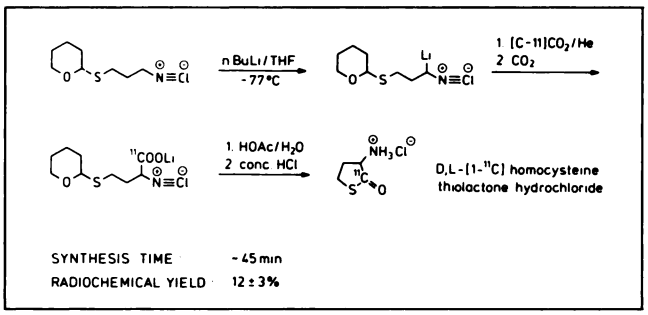

FIGURE 2. Synthesis of ^{11}C-labeled D,L-homocysteine thiolactone.

was stopped by heating. From the supernatant (10,000 g), 100–150 μl were taken for measurement of SAH by HPLC (*4*). To permit quantification, standard solutions of homocysteine (0.6, 6, 60 and 600 μ*M*) were treated in parallel.

Chemicals

Erythro-9-(2-hydroxy-3-nonyl)adenine (EHNA) was a gift from Dr. T. P. Zimmerman, Wellcome Research Laboratories, Research Triangle Park, NC. Sodiumpentobarbital was bought from La Societe Ceva, Neuilly-sur-Seine, France. DL-homocysteine thiolactone was obtained from Sigma, München, Germany. SAH and adenosine were purchased from Boehringer, Mannheim, Germany. All other reagents were supplied by Merck, Darmstadt, Germany.

Statistics

Data are given as mean values ± s.d. Radioactivity concentrations of different regions of interest were compared using Student's t-test for paired data. A p value of 0.05 was considered significant. Regression analyses were performed based on the individual determinations.

RESULTS

The kinetics of the plasma homocysteine and radioactivity concentrations were determined in three of four dogs in which 1-[^{11}C]-DL-homocysteine thiolactone was given i.v. over 1 min at a dose of 30 mg/kg (5–27 mCi). While plasma homocysteine increased from 2.5 ± 0.5 to 306 ± 89 μ*M* (n = 3; Fig. 3), the radioactivity concentration in blood plasma was 2.80 ± 0.35 μCi/cm^3 after 5 min. The consecutive decrease in the plasma homocysteine and radioactivity concentration showed a similar time course (Fig. 3), with $T_{½}$ being 28 and 37 min, respectively. In each experiment (n = 3), the plasma radioactivity concentration was linearly related to the plasma homocysteine concentration (r = 0.993, n = 15; r = 0.996, n = 15; r = 0.947, n = 7). In two further experiments, infusion of 1-[^{11}C]-DL-homocysteine thiolactone at a dose of 10 mg/kg (9–12 mCi i.v. over 1 min) gave a plasma radioactivity concentration of 2.08 μCi/cm^3 at 5 min. The plasma concentration of homocysteine was 75 μ*M* after 5 min and 44 μ*M* after 60 min (data are mean values from two experiments).

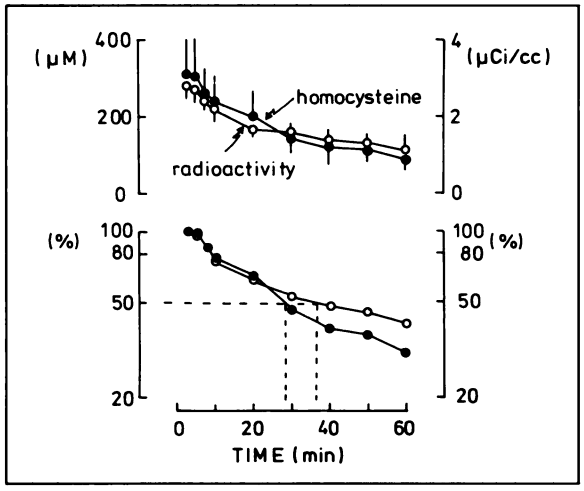

FIGURE 3. Effects of 1-[^{11}C]-DL-homocysteine thiolactone (5–27 mCi, 30 mg/kg), given over 1 min i.v., on the radioactivity and homocysteine concentration in dog plasma (upper panel: linear plot; lower panel: logarithmic plot). The dotted lines point to the $T_{½}$ for the homocysteine and the radioactivity concentration which were 28 and 37 min, respectively. Data summarize three experiments (mean ± s.d.).

Table 1 summarizes the body distribution of radioactivity 60 min after infusion of 15.3 mCi 1-[^{11}C]-homocysteine thiolactone (30 mg/kg i.v.), as assessed by PET. The highest radioactivity concentration was found in the bladder and the kidney followed by the liver, bone marrow, heart and skeletal muscle. The radioactivity concentration of the blood pool was similar to that of nonischemic heart muscle.

Figure 4A shows a representative tomogram for an experiment in which 1-[^{11}C]-homocysteine thiolactone was infused 5 min after occlusion of the left anterior descending coronary artery. The tomogram is based on the summarized radioactivity concentration between 10 and 60 min. Low radioactivity concentrations were found in lung, mediastinum and thoracic wall, well contrasted by the concentrations of heart and spine. From the slice shown at a higher magnification in Figure 4B (same experiment), it is evident that the radioactivity concentration in the anterior left ventricular wall, the underperfused area as assessed with ^{99m}Tc-labeled microspheres and postmortem gamma counting, was specifically elevated. The ratio of the radioactivity concentration in the anterior and posterior left ventricular wall was 1.6, while the radioactivity concentration in the posterior wall and the blood pool (left ventricular cavity) was similar. A comparison of the blood plasma radioactivity concentration, measured in a well counter, with that of the nonischemic posterior wall determined by PET, revealed a ratio of 1.03 ± 0.14 (n = 19 determinations between 5 and 60 min after injection). The ratio of the radioactivity concentration between native blood and plasma was 0.90 ± 0.06 (r = 0.998, n = 30).

TABLE 1
Radioactivity Distribution After Infusion of 1-[^{11}C]-DL-Homocysteine Thiolactone

Organ	Radioactivity (% per liter organ)
Bladder	40.7
Kidney	27.2
Liver	12.9
Spinal bone	7.1
Heart muscle	6.5
Skeletal muscle	3.6
Blood pool	6.1

Local radioactivity concentration was measured by positron emission tomography 60 min after injection of 0.85 mCi/kg 1-[^{11}C]-DL-homocysteine thiolactone i.v. The data given for heart muscle refer to nonischemic myocardium.

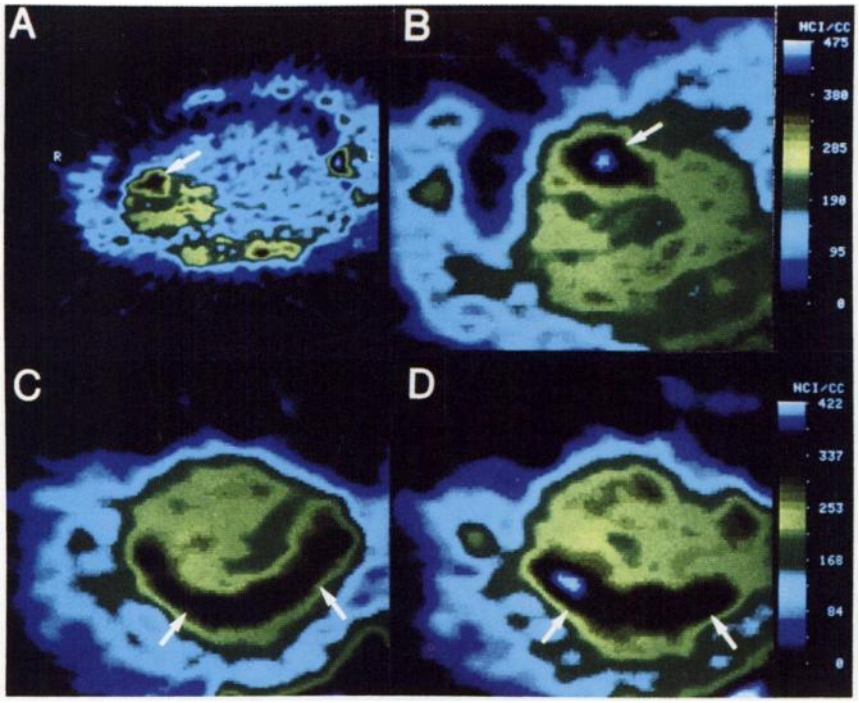

FIGURE 4. Tomograms showing the local radioactivity concentrations obtained 10-60 min following infusion of 1-[^{11}C]-DL-homocysteine thiolactone. (A) Slice in a horizontal plane of the thorax at a mid-myocardial level. The sternal region is on the left hand side, the red spot on the right hand side represents the spinal bone. The lower margin represents the dog's right thoracic wall. In the upper margin, the broken contour indicates the left sided thoracotomy. In the anterior mediastinum the heart is well contrasted by the surrounding tissue. An elevated radioactivity concentration is found in the perfusion area of the left anterior descending coronary artery (arrow). (B) Magnification of the cardiac region taken from the experiment shown under A. The arrow points to the ischemic region, the perfusion area of the left anterior descending artery. (C and D) Local radioactivity concentration during underperfusion of the posterior left ventricular wall (arrows). Two adjacent slices of a representative experiment are shown.

Taking into account the hematocrit and the fractional volume of water in erythrocytes (0.737) (*13*), the average ratio of the red blood cell and plasma concentration was 1.05.

Figures 4C and 4D show tomograms from an experiment in which the circumflex coronary artery was stenosed. This intervention decreased systolic/diastolic distal coronary pressure from 122 ± 5/104 ± 88 mmHg to 56 ± 3/23 ± 3 mmHg, but did not change mean aortic blood pressure (111 ± 6 mmHg) or heart rate (124 ± 8 bpm). Five minutes after setting the coronary stenosis 1-[^{11}C]-homocysteine thiolactone was given as outlined before. While the radioactivity concentration in the anterior left ventricular wall and the blood pool were similar, it was elevated in the posterior left ventricular wall, the perfusion area of the left circumflex artery in the dog. The underperfusion was verified with ^{99m}Tc-microspheres and postmortem gamma counting.

Figure 5A shows a representative time-activity curve for an experiment with circumflex underperfusion. In these experiments (n = 3), the radioactivity concentrations in the blood pool, the anterior and the posterior left ventricular wall were 1572 ± 996, 1628 ± 1165 and 1798 ± 1302 nCi/cm^3, equivalent to 9.28 ± 1.42, 8.96 ± 2.91 and 9.87 ± 3.05% of the injected dose per 1 liter of tissue 5 min after 1-[^{11}C]-homocysteine thiolactone. These concentrations were not significantly different from each other. Between 20 and 60 min, the radioactivity concentration was highest in the posterior left ventricular wall (Fig. 5A). During this time interval, the average concentrations in the blood pool, the anterior and the posterior left ventricular wall were 852 ± 511, 863 ± 520 and 1101 ± 670 nCi/cm^3, respectively, equivalent to 5.20 ± 0.40, 5.24 ± 0.41 and 6.61 ± 0.91% of injected dose per 1 liter ($p \leq 0.05$ posterior versus anterior left ventricular wall). The ratio of the radioactivity concentration in both myocardial regions averaged 1.4 after 60 min (Fig. 5B). The interindividual

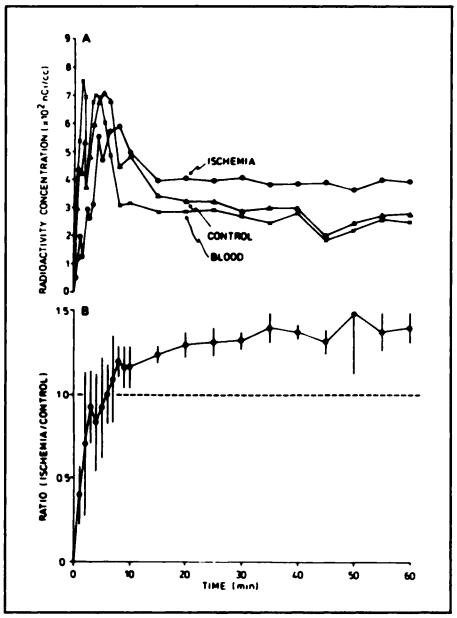

FIGURE 5. (A) Time-activity curves for ischemic and nonischemic (control) myocardium as well as blood pool. Data are from one representative experiment in which mean peripheral coronary perfusion pressure in the circumflex coronary artery was 40 mmHg. (B) Ratio of the radioactivity concentration between ischemic and nonischemic myocardium. Data summarize three experiments (mean ± s.d.).

reproducibility was good as indicated by the small standard deviations.

In the two experiments in which homocysteine carrier was administered in a lower concentration (10 mg/kg i.v.) plasma homocysteine was below 100 μM and the radioactivity concentrations in the anterior (control) and the posterior (ischemic) left ventricular wall were not different, although a comparable degree of coronary stenosis was imposed. Five minutes after 1-[^{11}C]-homocysteine thiolactone administration, the respective radioactivity concentrations for the blood pool, the anterior and the posterior left ventricular myocardium were 7.54, 9.88 and 9.18% of the injected dose per 1 liter, respectively. Between 20 and 60 min, the respective values were 5.12, 5.97 and 5.77% (average values from two experiments).

Figure 6 shows the time course of the radioactivity concentration of the SAH fraction in the ischemic myocardium after infusion of 20 μCi [^{35}S]-L-homocysteine thiolactone. While the total radioactivity concentration of the acid extract continuously fell after the end of homocysteine infusion, the radioactivity of the SAH fraction progressively increased. Thus, 20 min after homocysteine infusion, almost 60% of the total acid extractable radioactivity was recovered in the SAH fraction. In the nonischemic area, however, the radioactivity concentration associated with the SAH fraction remained low and was 1.9% after 30 min.

DISCUSSION

Adenosine is a locally acting metabolite, the formation of which is tightly linked to cardiac energy metabolism (*14*). Adenosine is believed to serve several important functions in the normal and diseased heart: regulation of coronary blood flow (*1,2*), mediation of the hypoxia-induced reduction of AV-node transmission (*15*), protection of the heart from sympathetic overstimulation (*16*) and reduction of infarct size due to inhibition of neutrophil-mediated injury to endothelial cells (*17,18*). From a teleologic point of view, all these actions of adenosine help to balance myocardial oxygen demand and supply via the coronary circulation. Adenosine has therefore been proposed to be a homeostatic metabolite which can adjust energy expenditure to oxygen supply at the local level (*19*). The most severe stimulus of cardiac adenosine production is ischemia.

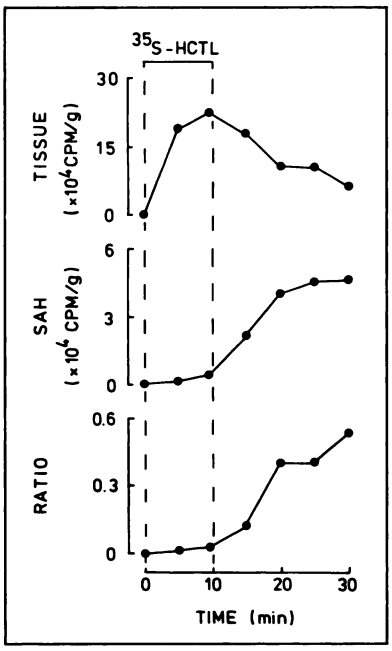

FIGURE 6. Effects of [^{35}S]-DL-homocysteine thiolactone (^{35}S-HCTL, 30 mg/kg, 20 μCi i.v.) on the ^{35}S concentration of the acid tissue extract (TISSUE), the SAH fraction (SAH) and the ratio of both fractions in the ischemic region.

This study demonstrates the feasibility of imaging enhanced concentrations of adenosine with PET using 1-[^{11}C]-DL-homocysteine thiolactone as precursor. The technique is based on the kinetic properties of SAH-hydrolase, a strictly cytosolic enzyme (*10*), which catalyzes the formation of SAH from adenosine and homocysteine (Fig. 1). At saturating homocysteine concentrations, the rate limiting factor in this reaction is the free adenosine concentration. Plasma concentrations of L-homocysteine are normally in the low micromolar range (*20*). In order to favor the net synthesis of SAH, we increased the plasma concentration of L-homocysteine to about 300 μM (Fig. 3). The consecutive decrease of the plasma homocysteine concentration (Fig. 3) may explain the steady-state radioactivity ratio relating ischemic-to-nonischemic tissue after about 20 min (Fig. 5B). At this point, plasma homocysteine decreased below 200 μM, the K_m-value of the enzyme. An alternative explanation for the steady-state radioactivity concentration after 20 min is that the metabolic parameters only transiently changed during the underperfusion, although the degree of stenosis was tightly controlled. This view is suggested by a recent study, which shows that during myocardial ischemia phosphocreatine levels may fall initially, but recover at later time intervals (*21*). Similarly, in the case of adenosine, we have observed a transient formation during demand ischemia (*5*). Knowledge of the kinetics of plasma homocysteine determined in the present study permits the design of future experiments that specifically address the kinetics of regional adenine nucleotide depletion/adenosine formation during myocardial underperfusion.

After infusion of 1-[^{11}C]-homocysteine thiolactone in the presence of a coronary stenosis, the early radioactivity concentration of the nonischemic myocardium was similar to that determined for the blood pool, while the underperfused myocardium showed a lower maximum (Fig. 5A). Multiple-indicator-dilution experiments reveal a permeability-surface area (PS) product for homocysteine thiolactone of 4.8 $ml \cdot min^{-1} \cdot g^{-1}$ (*22*). At a high PS-to-flow ratio, flow predominantly controls extraction. Because blood flow of the underperfused resting myocardium is less than 0.5 $ml \cdot min^{-1} \cdot g^{-1}$, i.e., less than one-tenth of the above PS value, the higher initial radioactivity concentration of the nonischemic myocardium may reflect the higher perfusion of this region.

In the present study, we used 1-[^{11}C]-DL-homocysteine thiolactone, a racemic mixture of the biologically active L-form and the inactive D-form. Our experiments with both isomers show that SAH-hydrolase only accepts L-homocysteine. Even after 1 hr incubation of both isomers in human and rat blood at concentrations of 160 and 800 μM, in vitro SAH formation with D-homocysteine was only 6.6 ± 1.6% of that obtained with L-homocysteine. This suggests that isomeric conversion of both forms is small. In future PET studies, the signal-to-noise ratio may therefore be considerably improved after appropriate separation of the racemic mixture.

The biodistribution of homocysteine thiolactone determined with PET in the dog (Table 1) is comparable to that determined in guinea pigs. Using [^{35}S]-L-homocysteine thiolactone (7 μCi/kg; 10 μg/kg over 3 min i.v.), we found after 30 min in guinea pig liver, kidney, heart, blood plasma and skeletal muscle 0.78 ± 0.13, 0.60 ± 0.04, 0.32 ± 0.06, 0.24 ± 0.01 and 0.13 ± 0.04% of the injected dose per g of tissue (n = 5). Table 1 indicates that most of the infused homocysteine is excreted by the kidneys into the urine. Compared with cardiac tissue the liver exhibited a higher radioactivity concentration, which is consistent with a higher SAH-hydrolase activity in this organ (*10*). Another consistent finding in all experiments was that radioactivity accumulated in the spinal bone (Fig. 4). There are several explanations for this finding. Most simply, the hemopoietic cells of the bone marrow may be rich in SAH-hydrolase activity or normally contain high levels of adenosine. Alternatively, other metabolic routes of conversion of homocysteine, e.g., to cysteine or methionine, may be more active in this tissue. There is, however, no information presently available to decide between these different possibilities.

The experimental condition of a coronary stenosis was chosen because it may closely resemble the hemodynamic situation in patients with coronary artery disease. At the degree of stenosis used in the present study, the coronary dilator reserve is almost exhausted, myocardial shortening, oxygen consumption and lactate extraction are diminished (*23*) and succinate is released (*24*). On the other hand, global cardiac function is still preserved. In this situation adrenergic stimulation of the heart may result in severe ischemia (*23*). For an average distal coronary pressure of 40 mmHg, we have previously shown that the free cytosolic adenosine concentration was steeply increased, while the total amount of adenine nucleotides was largely preserved (*4*).

The use of adenosine as a sensitive marker of ischemia in humans (*6*) rests on the highly different tissue concentrations of both metabolites. Tissue levels of ATP are usually about 4000 to 6000 nmol/g, while free adenosine levels are below 0.1 nmol/g (*8*). Thus, small changes in ATP give rise to large changes in the degradative product adenosine and this signal can now be picked up with labeled L-homocysteine using PET. The SAH-technique has the additional advantage that the kinetic approach of SAH accumulation leads to an augmentation of the original signal with time (*4,8*). Although the SAH-method is directly dependent on adenosine, this technique equally well reflects changes in local ATP.

An alternative method of noninvasive assessment of tissue energetics is provided by phosphorus magnetic resonance imaging (MRI) spectroscopy (*25*). The applicability of this technique to the ischemic human heart was recently demonstrated (*26*) although volume selective measurement in different areas of the heart is still a major problem. On the other hand, phosphorus MRI spectroscopy permits repetitive scanning of tissue high energy phosphates, thereby providing considerable temporal resolution. The SAH technique integrates the signal of free adenosine over time; the spatial resolution is good as the tomograms in Figure 4 demonstrate. The SAH technique may therefore complement phosphorus MRI spectroscopy measurements which provide information on energetics with high temporal, but less spatial resolution.

Differently labeled metabolites have been used to study the metabolic consequences of myocardial underperfusion. During ischemia, [^{11}C]palmitic acid clearance is significantly reduced (*27,28*), and the uptake of 17-[^{123}I]-iodoheptadecanoic acid is reduced (*29*), while uptake of [^{18}F]deoxyglucose may be elevated (*30*). This indicates that oxidative metabolism is suppressed and lactate formation from glucose may become more important. Previous PET studies, however, did not allow us to directly address the catabolism of high energy phosphates. The use of ^{11}C-labeled homocysteine may be suited to close this gap in the noninvasive assessment of in situ metabolism.

SAH-hydrolase is an enzyme found in sufficient activities in all organs studied (*10*), including the human heart (*31*). In combination with PET, the SAH technique may, therefore, be used as an important and new tool to assess the different regulatory roles of this nucleoside in various organs (*32*). In addition, our studies show that in the heart SAH should be a suitable biochemical marker by which a deterioration of tissue oxygenation or energy state can be monitored using 1-[^{11}C]-homocysteine thiolactone and PET.

ACKNOWLEDGMENTS

The authors wish to acknowledge the continuous financial support provided by a grant of the Deutsche Forschungsgemeinschaft within the Sonderforschungsbereich 242. Dr. A. Deussen is recipient of a Heisenberg-fellowship of the Deutsche Forschungsgemeinschaft (grant De-360/4.1). Dr. M. M. Borst was supported by a training grant from the Deutsche Forschungsgemeinschaft (Bo-813/1.1).

Part of this work was presented in abstract form at the 63rd annual fall meeting of the American Heart Association, Dallas, Texas, November 12–15, 1990.

REFERENCES

1. Berne RM. Cardiac nucleotides in hypoxia: possible role in regulation of coronary blood flow. *Am J Physiol* 1963;204:317–322.
2. Gerlach E, Deuticke B, Dreisbach RH. Der Nukleotid-Abbau im Herz-

muskel bei Sauerstoffmangel und seine mögliche Bedeutung für die Koronardurchblutung. *Naturwissenschaften* 1963;50:228–229.
3. Smolenski RT, Schrader J, deGroot H, Deussen A. Oxygen partial pressure and free intracellular adenosine of isolated cardiomyocytes. *Am J Physiol* 1991;260:C708–C714.
4. Deussen A, Borst M, Kroll K, Schrader J. Formation of S-adenosylhomocysteine in the heart. II: a sensitive index for regional myocardial underperfusion. *Circ Res* 1988;63:250–261.
5. Deussen A, Walter C, Borst M, Schrader J. Transmural gradient of adenosine in canine heart during functional hyperemia. *Am J Physiol* 1991; 260:H671–H680.
6. Fox AC, Reed GE, Glassman E, Kaltman AJ, Silk BB. Release of adenosine from human hearts during angina induced by rapid atrial pacing. *J Clin Invest* 1974;53:1447–1457.
7. Olsson RA, Bünger R. Metabolic control of coronary blood flow. In: Sonnenblick EH, Lesch M, eds. *Progress in cardiovascular diseases.* vol. 29. Grune & Stratton; New York: 1987:369–387.
8. Deussen A, Borst M, Schrader J. Formation of S-adenosylhomocysteine in the heart. I: an index of free intracellular adenosine. *Circ Res* 1988;63: 240–249.
9. Walker RD, Duerre JA. S-adenosylhomocysteine metabolism in various species. *Can J Biochem* 1975;53:312–319.
10. Ueland PM. Pharmacological and biochemical aspects of S-adenosylhomocysteine and S-adenosylhomocysteine hydrolase. *Pharmacol Rev* 1982; 34:223–253.
11. Hamacher K, Hanus J. Synthesis of 1-[^{11}C]-D,L-homocysteine thiolactone: a potential tracer for myocardial ischemia using PET. *J Lab Compds Radiopharm* 1989;27:1275–1283.
12. Rota-Kops E, Herzog H, Schmid A, Holte S, Feinendegen LE. Performance characteristics of an eight-ring whole body PET scanner. *J Comput Assis Tomogr* 1990;14:437–445.
13. Effros RM, Chinard FP. The in vivo pH of the extracellular space of the lung. *J Clin Invest* 1969;48:1983–1996.
14. Bünger R, Soboll S. Cytosolic adenylates and adenosine release in perfused working heart. Comparison of whole tissue with cytosolic non-aqueous fractionation analyses. *Eur J Biochem* 1986;159:203–213.
15. Belardinelli L, Belloni FL, Rubio R, Berne RM. Atrioventricular conduction disturbances during hypoxia: possible role of adenosine in rabbit and guinea pig heart. *Circ Res* 1980;47:684–691.
16. Schrader J, Baumann G, Gerlack E. Adenosine as an inhibitor of myocardial effects of catecholamines. *Pflügers Arch* 1977;372:29–35.
17. Cronstein BN, Levin RI, Belanoff J, Weissman G, Hirschhorn R. Adenosine: an endogeneous inhibitor of neutrophil mediated injury to endothelial cells. *J Clin Invest* 1986;78:760–770.
18. Engler RL, Dahlgren MD, Morris DD, Peterson MA, Schmidt-Schoenbein GW. Role of leukocytes in response to acute myocardial ischemia and reflow in dogs. *Am J Physiol* 1986;251:H314–H323.
19. Schrader J. Adenosine: a homeostatic metabolite in cardiac energy metabolism. *Circulation* 1990;81:389–391.
20. Saetre R, Rabenstein DL. Determination of cysteine in plasma and urine and homocysteine in plasma by high-pressure liquid chromatography. *Anal Biochem* 1978;90:684–692.
21. Pantely GA, Malone StA, Rhen WS, et al. Regeneration of myocardial phosphocreatine in pigs despite continued moderate ischemia. *Circ Res* 1990;67:1481–1493.
22. Grunbaum Z, Kroll K, Greene J, Rasey JS, Krohn KA. Synthesis and radiobiological applications of [^{35}S]L-homocysteine thiolactone. *Nucl Med Biol* 1990;17:473–478.
23. Heusch G, Deussen A. The effects of cardiac sympathetic nerve stimulation on the perfusion of stenotic coronary arteries in the dog. *Circ Res* 1983; 53:8–15.
24. Wiesner R, Deussen A, Borst M, Schrader J, Grieshaber MK. Glutamate degradation in the ischemic dog heart: contribution to anaerobic energy production. *J Mol Cell Cardiol* 1989;21:49–59.
25. Kantor HL, Briggs RW, Metz KR, Balaban RS. Gated in vivo examination of cardiac metabolites with ^{31}P nuclear magnetic resonance *Am J Physiol* 1986;251:H171–H175.
26. Bottomley PA, Herfkens RJ, Smith LS et al. Noninvasive detection and monitoring of regional myocardial ischemia in situ using depth-resolved ^{31}P NMR spectroscopy. *Proc Natl Acad Sci USA* 1985;82:8747–8751.
27. Lerch RA, Ambos HD, Bergman StR, Welch MJ, Ter-Pogossian MM, Sobel BE. Localization of viable, ischemic myocardium by positron emission tomography with ^{11}C-palmitate. *Circulation* 1981;64:689–699.
28. Schwaiger M, Schelbert HR, Keen R et al. Retention and clearance of C-11 palmitic acid in ischemic and reperfused canine myocardium. *J Am Coll Cardiol* 1985;6:311–320.
29. Freundlieb CH, Höck A, Vyska K, Feinendegen LE, Machulla HJ, Stöcklin G. Myocardial imaging and metabolic studies with 17-[^{123}I] iodoheptadecanoic acid. *J Nucl Med* 1980;21:1043–1050.
30. Schwaiger M, Brunken R, Grover-McKay M et al. Regional myocardial metabolism in patients with acute myocardial infarction assessed by positron emission tomography. *J Am Coll Cardiol* 1986;8:800–808.
31. Borst M, Deussen A, Schrader J. S-adenosylhomocysteine-hydrolase activity in human myocardium. *Cardiovasc Res* 1992;26:143–147.
32. Gerlach E, Becker BF, eds. *Topics and perspectives in adenosine research.* Berlin, Germany: Springer Verlag; 1987.

EDITORIAL

PET Imaging of Carbon-11-S-Adenosylhomocysteine: A Measure of Myocardial Energy Balance?

In the past decade, a variety of positron-emitting tracers have been developed, making it possible to study myocardial flow and metabolism noninvasively. The application of these tracers in man has expanded our understanding of the pathophysiological processes associated with ischemic heart disease. Myocardial blood flow can be assessed in relative and absolute terms (*1–3*), and substrate utilization can be studied (*4*). During ischemia, acetate utilization diminishes in parallel with oxidative metabolism (*5*), the oxidation of palmitate diminishes (*6*), and the uptake of glucose is enhanced relative to blood flow (*7*). Other techniques permit the assessment of cardiac receptors (*8*) and tissue oxygenation (*9,10*). In the current issue of the *Journal*, Deussen and colleagues demonstrate the feasibility of an important and novel strategy for probing cardiac metabolism, namely the detection of increased cytosolic adenosine (*11*).

An abundant literature has shown that an imbalance between myocardial oxygen supply and utilization causes a net degradation of adenine nucleotides leading to increased cytosolic adenosine. Increased cytosolic adenosine cannot be measured directly because of intracellular compartmentalization (*12*). The administration of excess homocysteine causes the formation of s-adenosylhomocysteine (SAH) from adenosine, via the enzyme SAH hydrolase, at a rate that reflects the intracellular adenosine concentration. Therefore, measurement of SAH during the administra-

Received Aug. 14, 1992; accepted Aug. 14, 1992.

For reprints contact: Gary V. Martin, MD, Division of Cardiology (111c), Vetrans Affairs Medical Center, 1660 South Columbian Way, Seattle, WA 98108.